- Technical Paper -

BOND SPLITTING CAPACITY OF CORRODED REINFORCED CONCRETE MEMBERS

Aris ARYANTO[*1] and Yasuji SHINOHARA[*2]

ABSTRACT

An experimental study was conducted to evaluate bond splitting behavior of corroded longitudinal bars in reinforced concrete beam with non-corroded stirrups. The pull-out tests were carried out to investigate effect corrosion through electrochemical corrosion process on bond splitting capacity, bond-slip relations and mode of failure including the influence of stirrup, bar position, and concrete strength. The test results showed substantial contribution of stirrups on residual bond splitting capacity and found that lower bond strength and small slip at maximum bond stress for corroded bars.
Keywords: corrosion, bond splitting, bond-slip relations, and stirrups

1. INTRODUCTION

Bond splitting mechanism of steel bars in concrete for uncorroded bars has previously been investigated by several researchers [1,2]. It is also known that the presence of stirrups increase the bond splitting capacity of longitudinal reinforcement. However, a complex bond splitting mechanism occurs when the corrosion of reinforcement involves. A significant reduction of bond strength has been observed for corroded of steel bar without stirrups [3,4] with an increasing corrosion level, however, slight bond strength deterioration was observed when the stirrups have been introduced [3,5,6]. In natural environment, not only longitudinal bars may experience corrosion, but also it may occur on stirrups. The corrosion of stirrups may weaken the confinement of longitudinal bars by reducing in stirrups area, provoking extensive cover cracking [7] and diminishing of adhesion or interface friction between stirrups and surrounding concrete. The combined effect corrosion of longitudinal reinforcement and corroded stirrups has been investigated in a few studies [7]. In this study the effect of stirrups is evaluate using non-corroded stirrups insulated by vinyl taping. To simulate the reduction in stirrups area, a small stirrup ratio and with various configurations of spacing and bar arrangements were taken into consideration of specimen parameters. The use of non-corroded stirrups is intended to maintain the stirrups area while corrosion of longitudinal bar is occurred. The used of vinyl taping on stirrups may also simulate the reduction in adhesion and friction of interface between corroded stirrups and concrete.

The aim of this study is to investigate the bond splitting behavior of corroded reinforcements such as bond splitting capacity, mode of failure and bond stress-slip relationships. The relative influence of uncorroded stirrups, longitudinal bar position and concrete strength were experimentally investigated in this study. As the experimental database, the test results may help in establishing the bond deterioration model of corroded reinforcement with various confinement levels as well as in formulation of bond-slip model for assessing the structural behavior of corroded structures

2. EXPERIMENTAL PROCEDURE

2.1 Specimens and materials

Pullout tests using beam type were carried out to evaluate the bond splitting behavior of corroded reinforcements. The effect of actual confinement by means of stirrups including effect of different stirrup ratios and configurations was investigated. The bar position on beams i.e. corner or middle bars and its position to casting direction i.e. top or bottom in casting were also evaluated in this study. The effect of corrosion attacks were investigated by performing electrochemical corrosion program.

Six 220x400 mm rectangular beams were produced and tested. Each beam had two test regions, the corrosion and the non-corrosion regions having a similar bar arrangement (Fig.1). Therefore in total twelve specimens were tested. The specimen parameters are summarized in Table 1. In this study only longitudinal bars located at bottom side of beams were subjected to corrosion which has 400 mm of embedment length. On the right and the left side of embedment length the longitudinal bars were insulated using vinyl tape as non-corroded and un-bonded regions. The stirrups were also covered by vinyl tape to protect stirrup gages during concrete placing and accelerated corrosion process. Before the accelerated

*1   Dept. of Environmental Science and Tech., Tokyo Institute of Technology, JCI Student Member
*2   Associate Prof., Structural Engineering Research Center, Tokyo Institute of Technology, JCI Member

corrosion test, all specimens were cured for 28 days in the laboratory environment. Two concrete strengths of 24 and 48 N/mm² were used representing a normal and high strength concrete. In this case, the concrete was not poured from the top of beams but from side of beams. Thus, there are four bar positions in terms of casting direction. (T, CT, CB, B). The preheated high strength of steel bar was also selected for longitudinal bars to avoid the yielding before bond splitting failure. Two bar diameters of 19 mm and 22 mm were used for longitudinal bars. The average yield strength, tensile strength and elastic modulus were 1053, 1128 and 1.87 × 10⁵ N/mm² for D19 and 980, 1031 and 1.85 × 10⁵ N/mm² for D22, respectively. For stirrups, high strength steel bar were also used having average yield strength, tensile strength and elastic modulus were 1414, 1490, and 2.0 × 10⁵ N/mm², respectively.

2.2 Accelerated corrosion

An accelerated corrosion test through the electrochemical process was performed. The typical accelerated corrosion set up for all specimens is described in Fig.2. During accelerated corrosion process the specimens were placed on top of two supports and the tank containing 3% of NaCl solution was put below the specimen. The solution penetrated to the concrete through the water sponge. Thus, the corrosion attack took place from one direction. The longitudinal bars were corroded up to approximately 6% of corrosion weight loss where cover crack

width estimated larger than serviceability limit (e.g. ACI's crack width limit of 0.3-0.5mm). The cracking of cover was visually observed and the crack width at certain locations was frequently measured using digital microscope [8]. Furthermore, a constant 10 Volt from the power supply was charged and the current flowed on each bar was monitored and recorded using data logger.
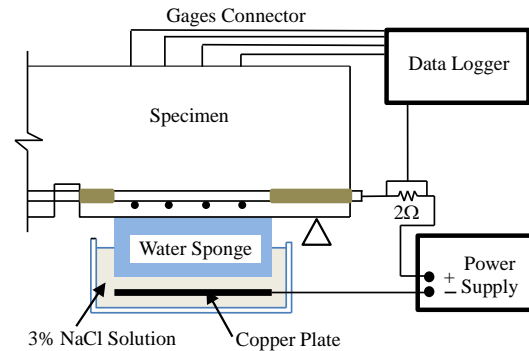
Fig. 2 Overview of accelerated corrosion setup

2.3 Pullout test

The specimens were tested in a simple three point loading. Because the beam has two test regions or specimens, corrosion and healthy regions, so after loading test was finished for one region, it was then continued with another test region in opposite loading directions by turning upside down. The outline of loading test set-up is described in Fig. 3. The loading

Table 1 Specimen's test parameters

No.	Specimens	Concrete Strength (N/mm²)	Longitudinal bar			Target Corrosion Rate (%)	Transverse bars	
			No. bar	dia. (mm)	Ratio		Bar	Ratio
1	4LT-∞S-NH	24	4	19	1.29%	0	0	0%
2	4LT-∞S-NC					6		
3	4L2T-200S-NH					0	2-U6@200	0.15%
4	4L2T-200S-NC					6		
5	4L2T-100S-NH					0	2-U6@100	0.29%
6	4L2T-100S-NC					6		
7	4L4T-200S-NH					0	4-U6@200	0.29%
8	4L4T-200S-NC					6		
9	3L2T-100S-NH		3	22	1.30%	0	2-U6@100	0.29%
10	3L2T-100S-NC					6		
11	4L2T-100S-HH	48	4	19	1.29%	0	2-U6@100	0.29%
12	4L2T-100S-HC					6		
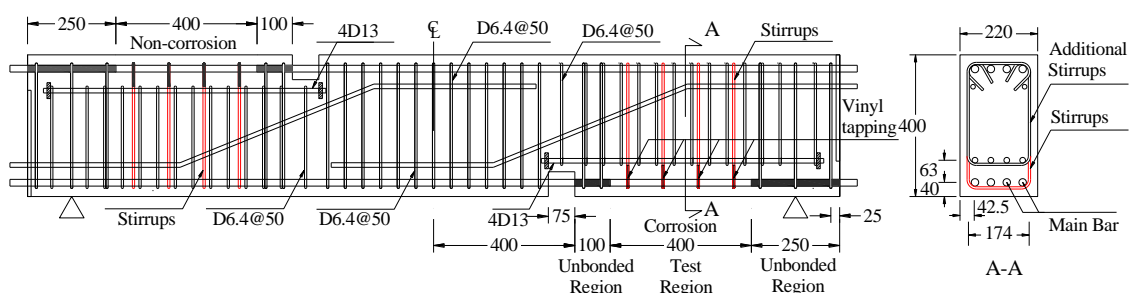
Fig. 1 Typical specimens and bar arrangements

was controlled by displacement and also it was controlled by measured strain in the longitudinal bar. In addition, the slip of each bar was measured using linear variable differential transformers (LVDT) which put at end of beams.
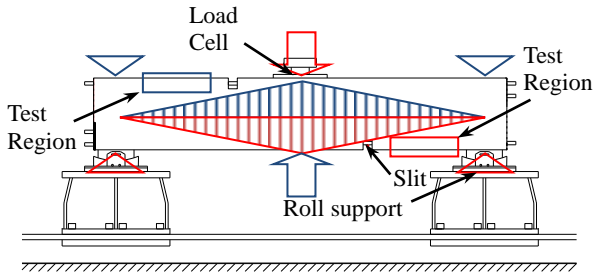
Fig.3 Overview of test setup and loading pattern

3. EXPERIMENTAL RESULTS

3.1 Corrosion weight loss

At the completion of pullout testing, the corroded longitudinal bars were removed from their concrete beams and the corrosion product was chemically cleaned by 10% diammonium hydrogen citrate solution, then it mechanically removed by steel wire brush and the weight loss was measured. The cleaning procedure of corrosion rust and the measurement of weight loss conformed to JCI-SC [9]. The summary of corrosion rate for each bar and the average in each beam are shown in Table 2.

From Table 2 it shows that the corrosion rates of each bar at a beam are different, although the output of current of each bar is relatively same. Larger corrosion rate was mostly obtained from the corner bar particularly bar located at top in casting (T). This trend was observed for all specimens. This can be attributed to the following: (a) crack due to corrosion mostly occur at edge of beam closed to edge bar, thus it allows water and oxygen to penetrate easily to the bars; (b) the bar located at top of concrete casting tends to have higher porosity than the bottom bar due to settlement of fresh concrete. The different of corrosion rate of each bar are relatively large compared to the estimated corrosion rate by Faraday's law (6%). However, if the average corrosion rate in one beam is compared to the estimated corrosion rate, the different is approximately 10%.

Table 2 Corrosion rate in weight loss (%)

No.	Specimen	Bar Location				Ave.
		T	CT	CB	B	
2	4LT-∞S-NC	10.6	4.7	3.8	5.6	6.2
4	4L2T-200S-NC	8.9	4.9	4.4	4.9	5.8
6	4L2T-100S-NC	8.2	4.4	5.4	6.3	6.1
8	4L4T-200S-NC	7.4	4.5	4.6	5.2	5.4
10	3L2T-100S-NC	7.4	3.9		6.3	5.8
12	4L2T-100S-HC	6.6	4.0	6.0	6.1	5.7

3.2 Crack patterns

The crack patterns and crack width at final accelerated corrosion or approximately 6% of corrosion loss are shown in Fig. 4(a). Generally, two major cracks were formed at the bottom cover of beams parallel to longitudinal bar.

(1) No.2 (4LT-∞S-NC)

(5) No.10 (3L2T-100S-NC)

(2) No.4 (4L2T-200S-NC)

(3) No.6 (4L2T-100S-NC)

(6) No.12 (4L2T-100S-HC)

(4) No.8 (4L4T-200S-NC)
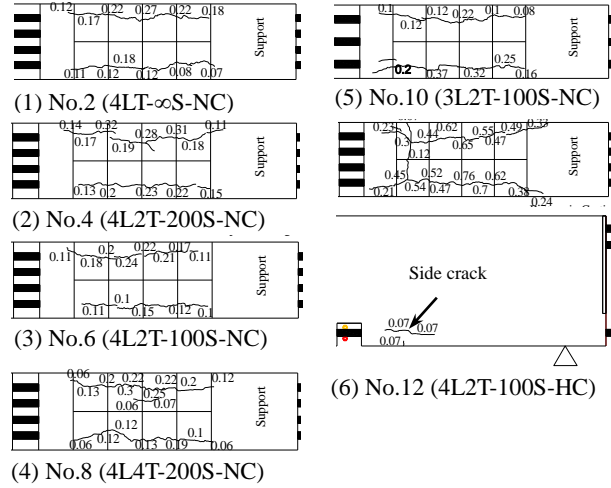
(a) Crack patterns at final accelerated corrosion

Healthy	Corroded
(1) No.1	(2) No.2
(3) No.3	(4) No.4
(5) No.5	(6) No.6
(7) No.7	(8) No.8
(9) No.9	(10) No.10
(11) No.11	(12) No.12
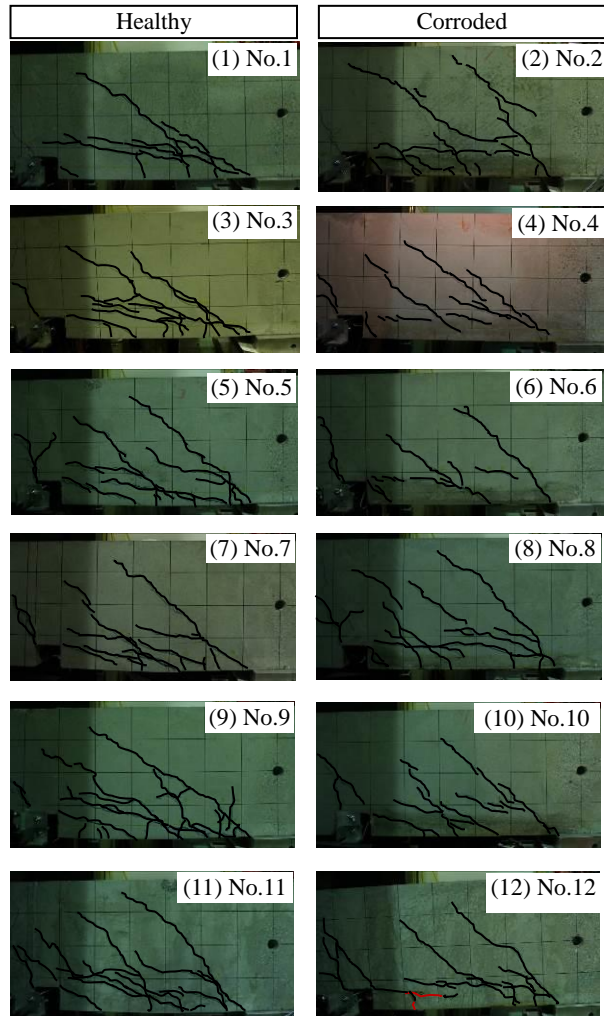
(b) Crack patterns at failure

Fig. 4 Crack patterns (a) at completion of accelerated corrosion, and (b) at failure

Typical crack patterns at bond splitting failure viewed from side of beams are described in Fig. 4(b). Different types of crack patterns were observed from the test results depending of presence and absence of corrosion and stirrups. For uncorroded (healthy) specimens without stirrups a small number of inclined cracks were formed starting from the bottom support as observed from the side view of beam (Fig. 4(b)(1)). The typical crack patterns for healthy specimens with stirrups were dominated by inclined cracks which have large number of cracks and more uniformly distributed along embedment length of longitudinal bars than specimen without stirrups as shown in Fig. 4.As shown in Fig 4 typical crack patterns for corroded specimens at side beam were also dominated by inclined cracks, however the cracks tend to form parallel to longitudinal bars or a smaller slope. Some of the parallel cracks were an extension from existing side cracks caused by corrosion. Based on the crack patterns generated on corroded specimens, the modes of failure for corroded specimens were mainly governed by splitting cracks parallel to longitudinal bars.

3.3 Bond stress-slip relationships

Fig.5 shows average bond stress-slip relationship for longitudinal bar in one specimen/beam. The bond stress was calculated from the tensile load acting on each longitudinal bar measured by strain gages attached on the longitudinal bar at slit and at unbounded regions divided by the surface area of longitudinal bar perimeter along the embedment length. Thus, the results are the average bond stress along embedment length. The dash line and the solid line in Fig. 5 show the bond stress-slip relationship of healthy and corroded specimens, respectively. The calculated bond strength for uncorroded (healthy) reinforcement based on the AIJ Guideline [10] as shown in equation (1) is illustrated by the dot line.

$$\tau_{max} = \alpha_t \left\{ (0.086b_i + 0.11)\sqrt{\sigma_B} + k_{st} \right\} \qquad (1)$$

where τ_{max}: maximum bond stress, α_t: effect of bar location, σ_B: concrete strength, b_i: effective concrete width, k_{st}: effect of stirrups.

For specimen without transverse bars, specimen No.1 and No.2, as shown in Fig. 5(a) the maximum bond stress (bond strength) of both specimens are relatively small around 2 N/mm^2 and it occurred at lower slip, less than 1 mm. Specimen No.2 has a slightly higher maximum bond stress than specimen No.1, the healthy specimen. This may be a possibility that the corrosion product filled the void at interface between reinforcement and concrete and enhanced the bond stress. However, after reaching maximum bond stress, the bond stress of specimen No.2 rapidly deteriorates due to influence of initial corrosion crack.

For specimens with transverse bars, the bond stress-slip relationship of specimen No. 3 to No. 12 (Fig. 5(b)-(f)) demonstrate that corrosion reduces the bond splitting capacity when comparing the bond strength between healthy and corroded specimens. It also shows that maximum bond stress for healthy specimens mostly occurred at larger slip more than 1 mm meanwhile for corroded specimens occurred at low slip smaller than 1 mm (brittle behavior).

As expected the presence of transverse bars increases the bond splitting capacity for healthy
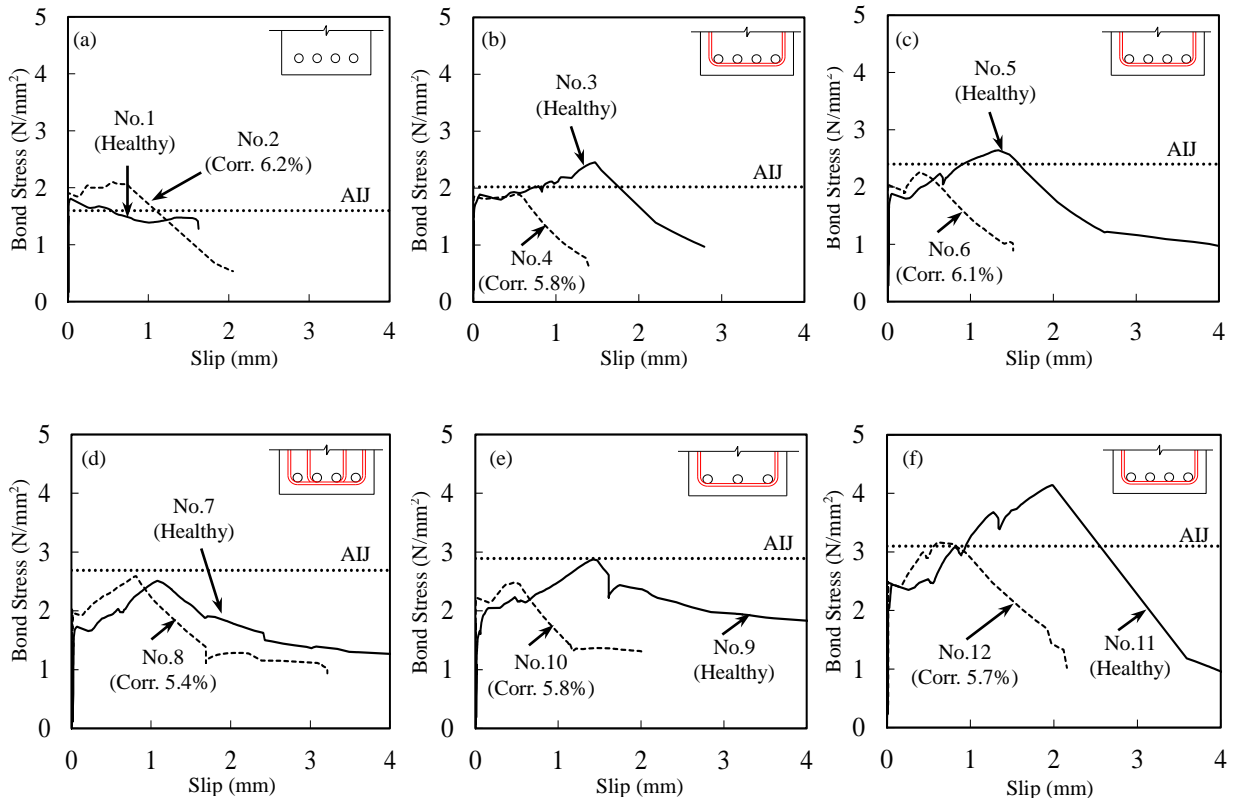
Fig. 5 Average bond stress-slip relationship

specimens. An increase in transverse bars ratio also increases the residual bond strength for corroded specimens. Moreover, it also shows that the presence of transverse bars enables to maintain the bond stress after reaching maximum bond stress at least one third of maximum bond stress at larger slip as shown in Fig. 5. This indicates that the presence of transverse bars influence the bond stress-slip relationship for corroded RC members. In addition, the bond stress at beginning of slip approximately at slip = 0.02 mm is about 2 N/mm^2 as reported by Aryanto et al. [4].

The bond-slip relationship for specimen with high concrete strength as shown in Fig. 5(f) has a larger maximum bond stress than for normal strength specimens. The average maximum bond stress for high concrete strength is 4.1 N/mm^2 and 3.2 N/mm^2 for healthy and corroded bars, respectively. This indicates high contribution of concrete strength on bond capacity. Moreover, the slip at maximum bond stress is also larger than normal concrete strength. However, the bond stress decreases rapidly after the maximum bond stress to lead a brittle behavior.

In order to assess the structural performance of corroded RC members, it is necessary to develop the bond-slip model for corroded reinforcement to model the relation between steel bar and concrete. The shape of the bond stress-slip curve as well as the bond strength is assumed depending on the corrosion level. As observed from the experimental test, corrosion influences the bond stress–slip curve in the following manners (Fig. 6):

1) Maximum bonds stress decreases with an increasing corrosion level except in low level corrosion
2) The slip at maximum bond stress decreases as increase corrosion level
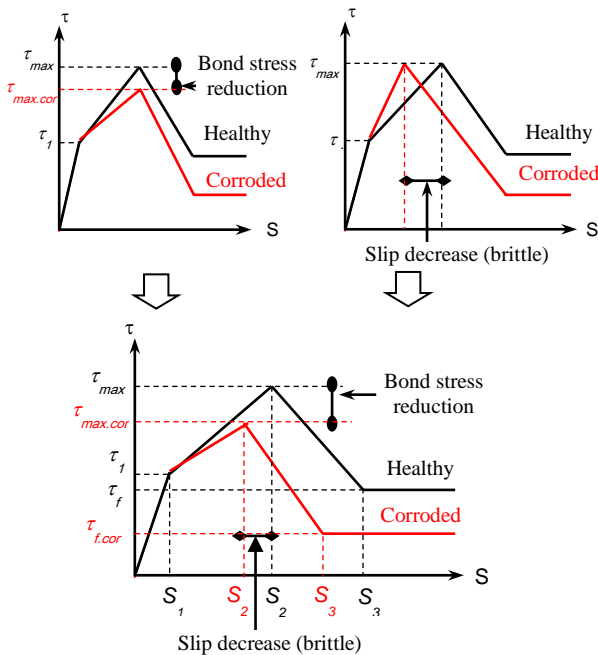
3) At early stage of bond stress-slip curve approximately up to 2 N/mm^2 or at slip = 0.02 mm, corrosion seems not changes the bond stress-slip curve.

3.4 Bond splitting capacity

Fig. 7 shows the test results in term of normalized maximum bond stress of each longitudinal bar with respect to maximum bond stress of bar located at bottom in casting (B) of healthy bar plotted against corrosion. For healthy bar, the different of bond splitting capacity between the bar located at bottom in casting (B) and top in casting (T) is approximately 5-15%. If bond strength is compared among longitudinal bars with respect to bar position in casting direction, for healthy specimens the bond strength of bars located at top (T) in casting have slightly lower bond value compared to bar located at bottom (B) in casting as shown in Fig. 7. This is can be due to larger porosity of concrete around bars located at top in casting. However, the effect of bar location on bond-slip relationships among corroded longitudinal bars seems insignificant. This can be attributed to cracks induced by corrosion and some of corrosion product may fill the concrete pore.

The average bond strength of each specimen normalized with respect to that of the healthy specimen without stirrups (No.1) plotted against stirrups ratio is shown in Fig. 8. The test data conducted by Morita et al. [11] which have stirrups ratio of 0.58 was added into the graph. From Fig. 8, for healthy specimens an increase of bond splitting capacity was observed with increasing stirrups ratio as illustrated by linear regression curve, solid black line. As indicated by a linear regression of corroded specimens, dash line, the test results showed bond deterioration due to effect of

Fig.6 Schematic view of bond-slip relationship for corroded reinforcement (Approx.6% of Corr. Loss)
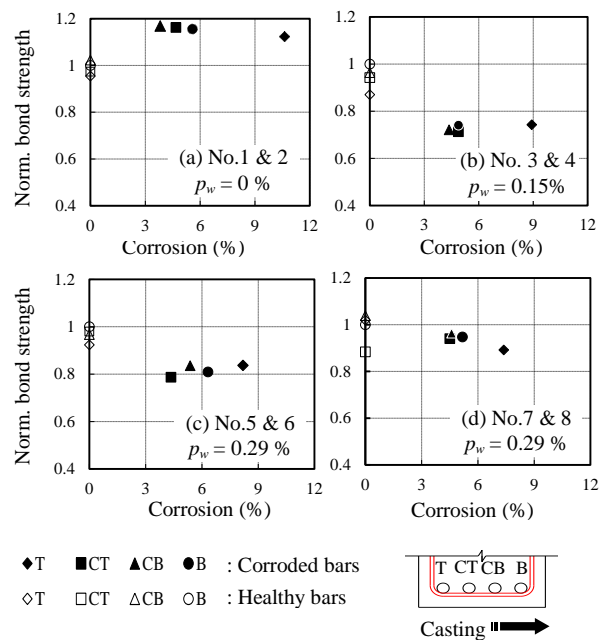
Fig.7 Normalized bond strength of each Bar with respect to that of healthy bar located at bottom in casting (B)

corrosion. However, as shown in Fig. 8 an increase in transverse bars ratio generated higher residual bond splitting capacity. This shows substantial contribution of confinement provided by transverse bars in corroded specimens. From Fig. 8 the decrease of bond strength of corroded longitudinal bar can be estimated for different confinement level or from the reduction area of transverse bar that might be occurred when transverse bar also experienced corrosion. Although the experimental data showed a scatter, the tendency of both effect of corrosion and transverse bars ratio was identified.
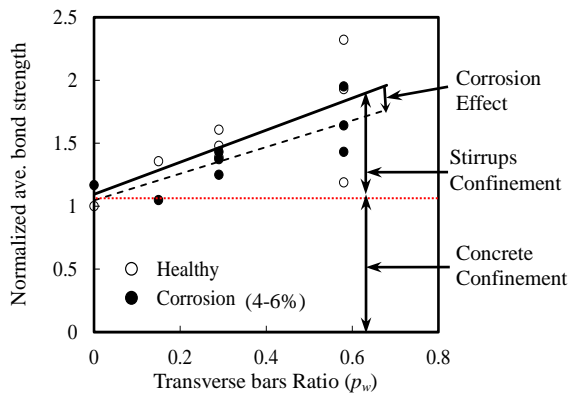
Fig.8 Normalized ave. bond strength with respect to that of the healthy specimen without stirrups

4. CONCLUSIONS

The pullout test on corroded RC members was performed to evaluate effect corrosion on bond splitting behavior of corroded RC members. The following conclusions can be drawn according to experimental results that discussed in this chapter.

1) Different behavior of bond stress-slip relationship between uncorroded and corroded reinforcement was observed from the experimental tests. Lower maximum bond stress and smaller slip at maximum bond stress were shown for corroded reinforcement and after reaching maximum bond stress, the bond rapidly deteriorated for corroded reinforcement.

2) An importance contribution of transverse bars to maintain residual bond splitting capacity for corroded specimens. The more transverse bar is provided, the higher residual bond splitting strength is generated.

3) A small effect of bar location in casting direction on the bond stress-slip relationships was observed for both corroded and healthy specimens.

4) The crack pattern at failure for corroded specimens mainly governed by splitting cracks parallel to longitudinal bar as an extension from the existing corrosion cracks and combined with a low slope of inclined splitting cracks. For healthy specimens, there was dominated by inclined splitting cracks

and the distribution of the inclined cracks was governed by the presence of stirrups.

ACKNOWLEDGEMENT

REFERENCES

1) Cairns, J. and Jones, K., "An Evaluation of The Bond Splitting Action of Ribbed Bars," Materials Journal., ACI, Vol.93, No.1, 1996, pp.10-19

2) Tepfers, R. A., "Cracking of Concrete Cover along Anchored Deformed Reinforcing Bars," Magazine of Concrete Research, Vol.31, No.106, 1979, pp.3-12

3) Al-Sulaimani, G. J. et al., "Influence of Corrosion and Cracking on Bond Behavior and Strength of Reinforced Concrete Members," Structural Journal., ACI, Vol.87, No.2, 1990, pp.220-231

4) Aryanto, A. and Shinohara, Y., "Influence of Bond-Slip Relationship and Tensile Strength on Bond Behavior between Corroded Bar and Concrete," J. Structural and Construction Engineering (Transaction of AIJ)., AIJ, Vol.78, No.685, 2013, pp.559-567

5) Al-Musallam et al., "Effect of Reinforcement Corrosion on Bond Strength," J. Construction and Building Materials, Vol. 10, No. 2, 1996, pp.123-129

6) Berra, M., Castellani, A. and Coronelli, D., "Steel-concrete Bond Deterioration due to Corrosion: Finite-element Analysis for Different Confinement Levels," Magazine of Concrete Research, Vol.55, No.3, 2003, pp.237-247

7) Hanjari, Z., Coronelli, D. and Lundgren, K., "Bond Capacity of Severely Corroded Bars with Corroded Stirrups," Magazine of Concrete Research, Vol.63, No.12, 2011, pp.953-968

8) Aryanto, A. and Shinohara, Y., "Cover Crack-width Propagation of Reinforced Concrete Members Induced by Corrosion," Proc. of the Japan Concrete Institute 2013, Vol.35, No.1, 2013, pp. 1123-1128.

9) JCI-SC., "Corrosion of Concrete Structures - Standards Test Method for Corrosion Protection," JCI, 1991

10) AIJ Committee., "Design Guidelines for Earthquake Resistant Reinforced Concrete Buildings Based on Inelastic Displacement Concept," AIJ, 1999

11) Morita et al., "Bond Behavior of RC Members with Corroded Longitudinal Reinforcement," Proc. Annual Meeting of AIJ, 2011, pp.411-414 (in Japanese)